Functional Composite Materials

RESEARCH Open Access

Optimization of process parameters of 3D printed thermoplastic elastomeric materials using statistical modeling with particular reference to mechanical properties and print quality

Pratiksha Awasthi[1†], Arun Kumar[2†], Pulak Mohan Pandey[2] and Shib Shankar Banerjee[1*]

Abstract

Additive manufacturing of thermoplastic elastomeric material (TPE) using direct ink writing (DIW) based printing technique opens new horizons for various applications. However, the most crucial process in DIW 3D printing is the optimization of printing parameters to obtain high-quality products both in terms of aesthetics and strength. In this work, statistical models were developed considering layer height, print speed, and, ink concentration to obtain the optimized print quality product from the blend of thermoplastic polyurethane (TPU)/epichlorohydrin–ethylene oxide–allyl glycidyl ether elastomer (GECO) based TPE materials. Experiments were designed according to the central composite design (CCD) scheme and the influence of input printing parameters on shrinkage and tensile strength was analyzed. The significance of each parameter was systematically studied using the response surface method. For both responses, shrinkage, and tensile strength, printing speed was found to be the most significant parameter. Ink concentration significantly affected tensile strength with a contribution of ~34%. On the other hand, the layer height, with a contribution of ~22% significantly affected the shrinkage behaviour of the 3D printed sample. Finally, multi-objective optimization was performed using a genetic algorithm to identify the optimal 3D printing parameters of the developed TPE materials.

Keywords Additive manufacturing, Thermoplastic elastomer, Direct ink writing, Central composite design

[†]Pratiksha Awasthi and Arun Kumar share equal authorship.

*Correspondence:
Shib Shankar Banerjee
ssbanerjee@mse.iitd.ac.in
[1]Department of Materials Science and Engineering, IIT Delhi, Hauz Khas 110016, New Delhi, India
[2]Department of Mechanical Engineering, IIT Delhi, Hauz Khas, New Delhi 110016, India

Introduction

Additive manufacturing is a rapidly growing technique that aids the fabrication of intricate or complex designed parts with the help of a computer-aided design (CAD) model [1–4]. A number of additive manufacturing techniques are currently available, including stereolithography, fused deposition modeling (FDM), direct ink writing (DIW), powder bed fusion, and, material jetting [5–8]. These techniques differ fundamentally in terms of feeding material, speed, and printing technology. On a commercial scale, FDM is a highly utilized additive manufacturing technique, however, the technique is challenging for printing soft polymeric material [9–11]. In the FDM process material in the form of a filament is fed with the aid of counter-rotating rollers into the heated liquefier head. The filament pushes the molten material from the heater head through the nozzle. For successful material extrusion through the nozzle, the filament should be able to withstand the pinching force exerted by the rollers and it should be rigid enough to exert a force to push the molten material. However, if the filament is soft in nature, it will not be able to withstand the pinching force. Moreover, soft filament will buckle causing poor material extrusion leading to poor part fabrication. Thus, the FDM process is incompatible for soft filament materials such as elastomers and thermoplastic elastomers [12, 13]. On the other hand, the DIW technique could be employed to print soft materials like elastomers or thermoplastic elastomers (TPEs) in liquid or semi-liquid phases [14–16].

TPEs are a hybrid polymer material consisting of a hard segment and a soft segment. This class of material is in high demand because of its easy processability like thermoplastics and rubber-like elasticity [17–21]. TPEs possess immense industrial importance due to their excellent processability, superior mechanical properties along with recyclability, and excellent price-performance balance [22–25]. As a bridge between thermoplastics and elastomers, TPEs are in great demand [26–28]. However, the manufacturing process of TPEs typically depends on conventional molding techniques. The use of TPEs could increase manifold with the introduction of additive manufacturing techniques for the production of TPE products. There are some commercial TPE filaments that are easy to print however, most of the soft TPE filaments are not compatible with commercial FDM 3D printers.

In the current work, the DIW technique was employed to print the soft TPE material prepared by melt blending of thermoplastic polyurethane (TPU) and epichlorohydrin–ethylene oxide–allyl glycidyl ether (GECO) rubber. The authors' in their previous work developed different blends of TPU and GECO and it was observed that the 50TPU/50GECO blend possessed better thermoplastic elastomeric properties [23, 29]. Therefore, in this work, a 50TPU/50GECO blend was utilized to prepare the ink sample using tetrahydrofuran as solvent and emphasized on development of statistical models and optimization of printing parameters to obtain optimum mechanical properties along with better print quality. The response surface method was used to develop a correlation between layer height, print speed, and ink concentration for tensile strength and shrinkage. Finally, multi-objective optimization was performed using a genetic algorithm to identify the optimal process parameters of the developed TPE materials.

Materials and methods

Materials

The thermoplastic polyurethane (TPU-HP 93 A 100) in granular form having a density of 1.13 g/cm^3 was obtained from Lubrizol Corp. (USA) and epichlorohydrin–ethylene oxide–allyl glycidyl ether, GECO (Hydrin T3000LL) having Mooney viscosity, ML_{1+4} at 100 °C 57 and density 1.28 g/cm^3 was purchased from Zeon Chemicals (USA). Tetrahydrofuran (THF) was purchased from ThermoFischer Scientific, USA.

Method

Preparation of 50TP/50G blend

A blend of 50TPU/50GECO (w/w) was prepared by melt blending technique in Haake Rheomix (350 ml, Haake OS Lab Mixer) equipped with roller-type rotors for 10 min at 140 °C and the rotor speed was 80 rpm. The 50/50 blend composition was selected due to its better thermoplastic elastomeric properties as reported in the author's previous work [23]. Prior to mixing TPU granules were kept in a hot air oven for 12 h at 80 °C for drying. During mixing, initially, TPU was incorporated in the roller and after proper melting, GECO was added and allowed to be mixed further.

DIW 3D printing

DIW-based additive manufacturing comprises of 3 steps as illustrated in Fig. 1. The first step in the DIW-based additive manufacturing process involves developing an input file with the information about the model to be 3D printed and the printing parameters [30]. The process begins with the development of a CAD model of the desired part using Solidworks version 2021. The developed CAD models are then tessellated which essentially involves the approximation of the part surface by triangles. The tessellated file is then further used for slicing with the aid of Prusa Slicer in which layer-by-layer material deposition information (print speed, raster angle, infill percentage, and, layer thickness) is stored in the form of a g-code file. This g-code file is ultimately transferred to the printer for printing the sample. The generated file is in the format of g-code and it is transferred to the printer. In step 2, polymeric ink was made

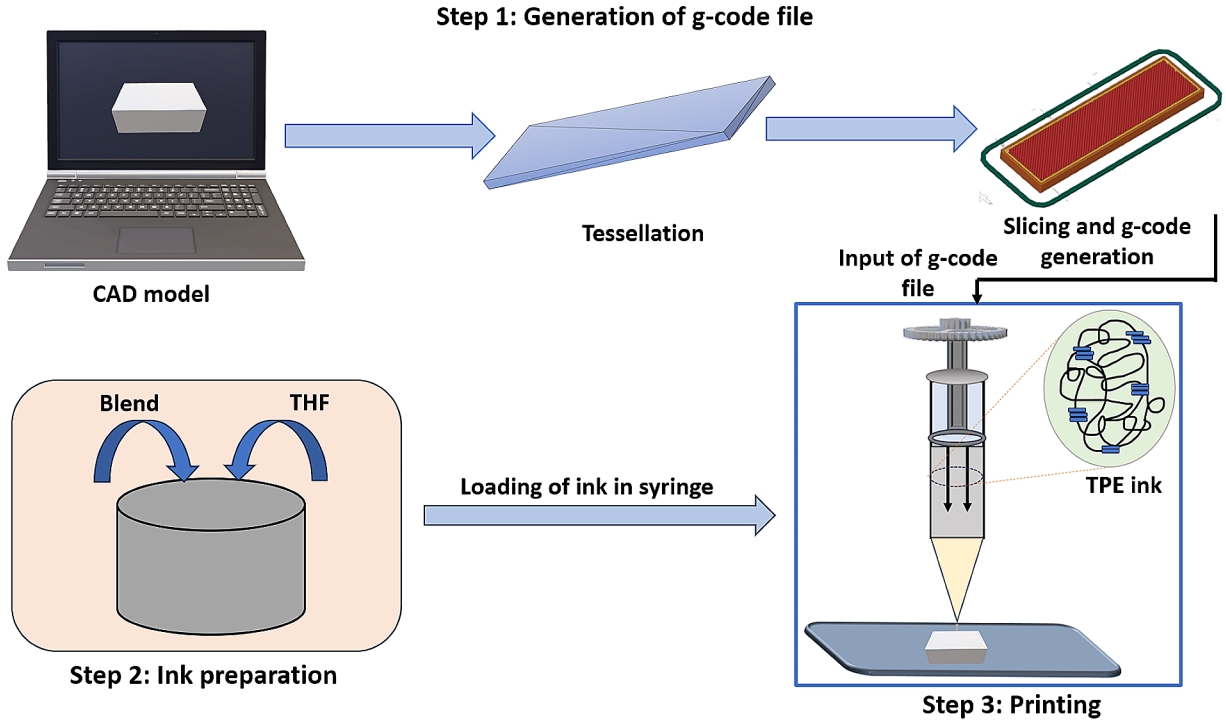

Fig. 1 Schematic illustration demonstrating the various steps involved in DIW-based additive manufacturing

Table 1 Process parameters along with their defined levels

Factors representation	Factors (unit)	Levels				
		−2	−1	0	1	2
X_1	Layer height (mm)	0.20	0.25	0.30	0.35	0.40
X_2	Print Speed (mm/s)	6.00	9.00	12.00	15.00	18.00
X_3	Ink Concentration (wt%)	10.00	15.00	20.00	25.00	30.00

by dissolving 50TPU/50GECO blend in THF in 10, 15, 20, 25, and 30 wt%, respectively. The polymeric ink was made by dissolving the polymer in THF in a high-shear mixer (HSM-100LSI, Ross Process Equipment Pvt. Ltd.) at room temperature. Then the ink was left for 10 min to remove the air bubbles generated due to the shearing action. The ink was transferred to the 10 mL luer-locked medical-grade syringe of 10 mL. Then in the last step, a syringe was clamped in the printer head (Alfatek Bio Bot Printer- Anga Pro). It regulates the material flow with the aid of a screw-type mechanism and deposits the ink in a layered manner according to the g-code on the petridish.

Selection of parameters for 3D printing

In the current study, three input parameters i.e. ink concentration (wt%), print speed (mm/s), and layer thickness (mm) having five levels (presented in Table 1) of all the parameters were selected for 3D Printing. In this study, response surface methodology (RSM) was adopted to evaluate the effect of input process parameters on the selected responses. The major advantage of RSM is that it can capture the non-linear effect of parameters [31]. Thus, five different levels of input parameters were selected based on the preliminary experiment, machine limitations, and reviewed literature.

Initially, to select the ink concentration different polymer to solvent ratio inks were prepared. It was noticed that parts 3D printed using ink having polymer content less than 10 wt% were not able to sustain the shape, as ink was highly flowable due to very low viscosity as could be seen from Fig. 2A. Whereas, the inks having polymer content more than 30 wt% possessed undissolved particles in the solution. Therefore, in this work ink concentration ranging from 10 wt% to 30 wt% was considered. For layer height, the range was selected between 0.2 mm and 0.4 mm. With the decrease in layer height, the amount of print time increased considerably. Additionally, it was observed in preliminary experiments that the nozzle was interfering with the deposited layer due to material over-deposition in layer height less than 0.2 mm which resulted in a poor sample fabrication, whereas, for higher layer height dimensional accuracy was not appropriate

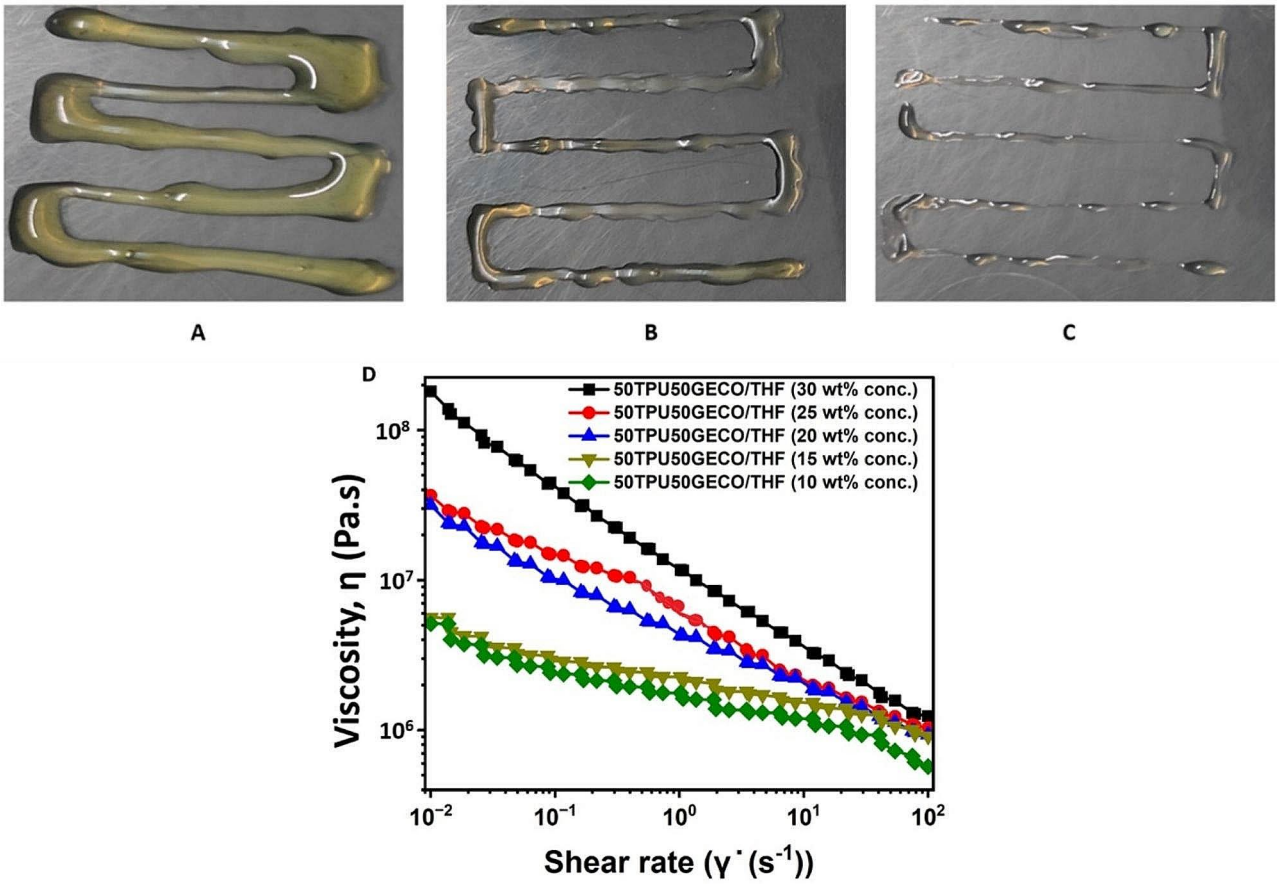

Fig. 2 (**A**) Printed sample demonstrating the distorted shape with less than 10wt% ink concentration, printed samples of 20 wt% ink at different print speeds, (**B**) 15 mm/s, (**C**) 20 mm/s and, (**D**) rheological behaviour of the ink (viscosity vs. shear rate)

[32]. So, based on these two observations i.e. print time and print quality the range for layer height was selected between 0.2 and 0.4 mm. Along with concentration and layer height, print speed was the third parameter considered in this work. Figure 2B and C demonstrate the dimensional stability of the deposited lines of 20 wt% ink with print speeds of 15 and 20 mm/s, respectively [33]. It could be observed that for a print speed of 20 mm/s, discontinuous or broken lines were obtained as the print head is moving comparatively faster. Whereas, continuous printed lines were obtained with a print speed of 15 mm/s. Figure 2D represents the rheological behaviour of the ink and it was observed that all the ink samples showed shear-thinning behaviour which is suitable for direct ink writing [34].

Characterizations

Rheology The rheological behavior of the developed inks was investigated using a parallel-plate rheometer (Anton-Paar 302 Rheometer) at room temperature. The diameter of the plates was 25 mm with a 0.3 mm gap between the parallel plates. The frequency sweep test was done in the frequency range of 0.01 to 100 rad/s with 1% strain throughout the test.

Mechanical testing Tensile testing of printed samples was performed on a universal testing machine (UTM Zwick Roell, 10 kN, Z010). The testing was done at ambient temperature with a crosshead speed of 200 mm/min.

Shrinkage Shrinkage in the printed sample was calculated following the CAD model. The thickness of the developed shape in the CAD model is 2 mm. However, it is known that due to the evaporation of the solvent in DIW-based printing, there is always a shrinkage in the printed sample. Samples were printed on the petri-dish and maximum shrinkage was obtained along thickness as shrinkage along length and width was restricted by the adhesion between printed the layer and surface of the petridish [35]. The thickness of the printed sample (T_{ACTUAL}) was measured with the aid of a vernier caliper and compared with the thickness of the CAD model (T_{CAD}). The percentage shrinkage was analyzed by the Eq. (1) [36]-

Table 2 Printing parameters along with responses of experimental trials

Experiment No.	Layer height (mm), X_1	Print speed (mm/s), X_2	Ink concentration (%), X_3	Shrinkage (%)	Tensile strength (MPa)
1	0.30	12	20	47.80	2.37
2	0.25	15	15	59.30	1.68
3	0.30	12	30	40.00	2.65
4	0.35	15	15	67.75	1.55
5	0.30	12	20	46.90	2.25
6	0.35	9	25	47.54	2.49
7	0.30	6	20	46.50	2.55
8	0.30	12	20	44.20	2.45
9	0.25	9	15	46.75	2.17
10	0.35	9	15	53.00	2.00
11	0.25	15	25	50.70	2.25
12	0.30	12	20	47.10	2.19
13	0.30	12	10	59.96	1.52
14	0.30	12	20	48.10	2.21
15	0.25	9	25	38.50	2.58
16	0.20	12	20	43.00	2.23
17	0.40	12	20	66.20	1.41
18	0.30	12	20	50.20	2.15
19	0.30	18	20	72.50	1.32
20	0.35	15	25	56.27	1.93

$$Shrinkage = \frac{T_{CAD} - T_{ACTUAL}}{T_{CAD}} \times 100 \quad (1)$$

Statistical modeling The investigation in the present work was carried out by following the central composite design (CCD) scheme to study the impact of various printing parameters on the output. CCD assists in generating the quadratic order equations for the responses for a broad range of factors with a limited number of trials [37]. Response surface methodology was needed for modeling and analyzing the selected printing process parameters on the quality of the 3D printed specimens. The range of the input parameters was predicted according to the previous studies and pilot experiments [12]. The regression equation for the response can be expressed in the form of Eq. (2) in terms of input process parameters [30]-

$$\widehat{y} = \alpha_0 + \sum_{i=1}^{k} \alpha_i X_i + \sum_{i=1}^{k} \alpha_{ii} X_i^2 + \sum_{i=1}^{k} \sum_{j>i}^{k} \alpha_{ij} X_i X_j + \epsilon \quad (2)$$

where, $\widehat{y}$ signifies the desired output, and k denotes the number of factors taken for the experiment. α_0, α_{ii} , and α_{ij} depict the regression coefficients, whereas ϵ shows the error term. X_i , X_i^2, and $X_i X_j$ are the linear, quadratic, and interaction terms of printing parameters, respectively.

Table 2 provides the set of experimental trials performed along with the obtained responses. Analysis of variance (ANOVA) tables having only significant terms (*p-value*<0.05) for the responses are given in Tables 3 and 4. The obtained regression equations for the responses are provided in Eqs. 3 and 4. The value of R-square (R^2) and Fisher's value (*f -value*) obtained through regression with the standard value (model and lack-of-fit) provides an estimation of the accuracy of the model.

$$Shrinkage = 117.7 - 298.3 \times X_1 - 5.54 \times X_2 - 0.921 \times X_3 + 655 \times X_1^2 + 0.3180 \times X_2^2 \quad (3)$$

Table 3 ANOVA analysis for shrinkage

Source	DF	Adj SS	Adj MS	F-Value	*P*-Value	R^2	Remarks
Model	5	1576.46	315.291	73.59	0	95.03%	$F_{0.05,5,14}$= 2.958
Linear	3	1325.7	441.9	103.13	0		$F_{model} > F_{0.05,5,14}$
Square	2	250.76	125.378	29.26	0		Model is adequate
Error	14	59.99	4.285				
Lack-of-Fit	9	40.92	4.546	1.19	0.446		$F_{0.05,9,14}$= 2.645
							$F_{lack\ of\ fit} < F_{0.05,9,14}$
Total	19	1636.44					Lack of fit is insignificant

DF: Degree of freedom, F-value: Fisher's value, Adj MS: Adjusted mean squares, Adj SS: Adjusted sum of squares

Table 4 Anova analysis for tensile strength

Source	DF	Adj SS	Adj MS	F-Value	*P*-value	R^2	Remarks
Model	5	2.88333	0.57667	35.46	0	90.07%	$F_{0.05,5,14}$ = 2.958
Linear	3	2.55117	0.85039	52.30	0		$F_{model} > F_{0.05,5,14}$
Square	2	0.33216	0.16608	10.21	0.002		Thus, model is adequate
Error	14	0.22764	0.01626				$F_{0.05,9,14}$ = 2.645
Lack-of-Fit	9	0.16044	0.01783	1.33	0.396		$F_{lack\text{-}of\text{-}fit} < F_{0.05,9,14}$
Total	19	3.11098					Thus, lack-of-fit is insignificant

DF: Degree of freedom, F-value: Fisher's value, Adj MS: Adjusted mean squares, Adj SS: Adjusted sum of squares

Table 5 Confirmatory experiments

S. No.	X_1 (mm)	X_2 (mm/s)	X_3 (%)	Shrinkage (%)		Tensile Strength (MPa)	
				Statistical	Experimental	Statistical	Experimental
1	0.35	12.00	15.00	59.03 ± 4.49	58.10	1.73 ± 0.27	1.92
2	0.30	15.00	20.00	57.19 ± 4.49	53.45	1.89 ± 0.27	2.04
3	0.35	9.00	20.00	51.01 ± 4.49	49.84	2.18 ± 0.27	2.38

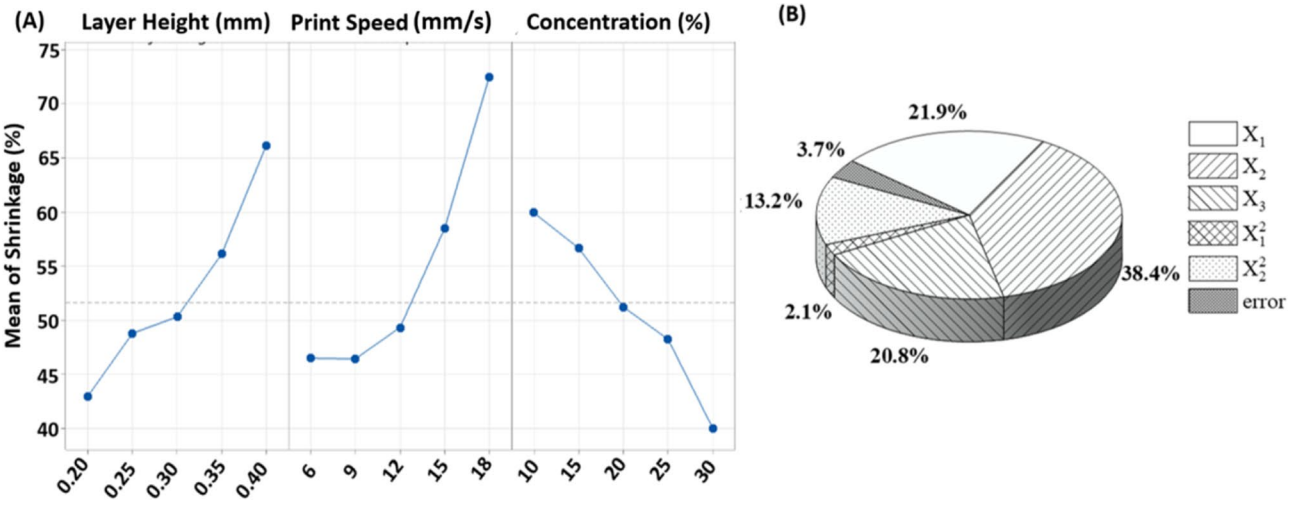

Fig. 3 Influence of printing parameters on shrinkage (**A**) Main effect plot and, (**B**) percentage contribution chart

$$Tensilestrength = -1.52 + 20.76 \times X_1 + 0.0973 \times X_2 + 0.05138 \times X_3 - 39.5 \times X_1^2 - 0.00778 \times X_2^2 \quad (4)$$

The accuracy of the models was investigated by the R^2 values and it was observed that the obtained R^2 values are 95.03% for shrinkage and 90.07% for tensile strength. The variation range for the predicted response was evaluated using Eq. (5)-

$$\widehat{y}_r = \widehat{y}_p + t\alpha_{/2,DF} \times \sqrt{V_e}\,(5) \quad (5)$$

where $\widehat{y}_p$ depicts the predicted value from regression of the response eq.; $t\alpha_{/2,DF}$ signifies the t-value at a significance level, α is 0.05 and DF is the degree of freedom for the experiments. The generated models were validated by doing confirmatory experiments provided in Table 5. The value ($\widehat{y}_r$) for the responses was predicted by Eq. (5) and it was noted that the observations were in good agreement with the generated statistical models.

Results and discussion

Influence of printing parameters on shrinkage

It was observed that shrinkage was highly influenced by layer height, print speed, and concentration of the ink. Materials deposition behaviour changes with change in layer height, print speed, and shrinkage [38]. Therefore, experiments were done to evaluate the effect of the above-mentioned process parameters on the shrinkage and are provided in Fig. 3A and B as the main effects plot and percentage contribution.

Influence of layer height

Layer height is the thickness of the individual deposited layers while printing. During slicing the build part is sliced in such a manner that the sum of the total deposited layers would be equal to the thickness of the sample to be printed. The deposition behaviour of the material changes with the change in the layer height [39]. In Fig. 3A it was identified that with enhancement in layer height, there is an increase in shrinkage from 43 to 67%. This could be due to the reason that samples printed with a lower layer height (0.2 mm) would accumulate more amount of material as compared to the samples printed with a higher layer height (0.4 mm). The increase in layer height resulted in a higher gap between the substrate and nozzle tip which leads to dragging of the material [38]. The dragging of the material at a higher layer height would led to the lower cross-sectional area of the printed material leading to a higher shrinkage effect [38].

Influence of print speed

In Fig. 3A-B it could be noticed that print speed is the most significant parameter that affects the percentage shrinkage of the developed 50TPU/50GECO blend. A change in print speed leads to a change in the deposition behaviour of the extruded material. It was found that the percentage of shrinkage increased as the print

speed increased, as less material was deposited on the print bed at a higher speed (18 mm/s) and more material was deposited on the print bed at a lower speed (6 mm/s). These observations were in line with the findings reported by Guo et al. [40]. In the contribution chart, Fig. 3B it could be observed that print speed contributed around 38%, which is higher than any other parameters. At higher print speed it was observed (Fig. 2C) that the lower material is deposited while printing which is due to the dragging of material resulting in higher shrinkage [41].

Influence of ink concentration

Ink concentration is the factor that influences (~21%) the shrinkage of the printed specimen. In Fig. 3A it could be noticed that the percentage of shrinkage decreased from ~60–40% as the ink concentration increased. This could be attributed to the fact that as the ink concentration increased, the relative amount of polymer content present in the prepared ink also increased. DIW technique involves the evaporation of the solvent, therefore, if the amount of solvent is higher in the ink concentration, then lower material will be deposited in the print bed once the solvent evaporates leading to a higher shrinkage. It can therefore be inferred that the higher the polymer content in the ink, the lower the shrinkage and vice versa.

Influence of 3D printing parameters on tensile strength

The printing process parameters such as print speed and, layer height strongly influence the material deposition behaviour which in turn governs the physical properties of the 3D printed part [42]. Thus, experiments were performed to determine the influence of layer height, print speed, and ink concentration and Fig. 4A and B represent the main effects plot and percentage contribution of significant factors for the tensile strength of the 3D printed samples. It could be observed that print speed, layer height, and ink concentration significantly affected the tensile strength. However, the print speed was the most significant parameter with a percentage contribution of around 37%.

Influence of layer height

Figure 4B suggests that layer height significantly influenced the tensile strength of 3D printed 50TPU/50GECO parts. It was observed that the value of tensile strength decreased from ~2.2 to 1.5 MPa with increasing the layer height from 0.2 to 0.4 mm. It was also observed that while material deposition with higher layer height, the effective distance between substrate and nozzle is high. Thus, when the material is deposited the cross-sectional area of the extruded material is reduced due to the phenomenon of dragging [40]. Moreover, the effective contact among the neighbouring deposited rasters also reduced drastically at larger layer heights leading to the presence of defects such as voids in the final sample. These observations are in line with the observations reported by Kandi et al. [30].. On the other hand, when the layer height is low (0.2–0.3 mm), the number of layers are higher which leads to higher interfacial fusion within the layers as compared to the samples printed with higher layer height (0.35 mm and 0.40 mm) [43].

Influence of print speed

It was identified that the tensile strength decreased significantly with the increase in print speed. These observations are in line with the previous literature [30]. At a higher speed (18 mm/s), the movement of the print head across the deposition bed is comparatively high which leads to improper deposition of layers and the deposited material is relatively less in amount hence causing gaps between the neighboring deposited layers and ultimately leading to poor fusion among the layers. In Fig. 4B, it was observed that print speed contributes around 37% on the

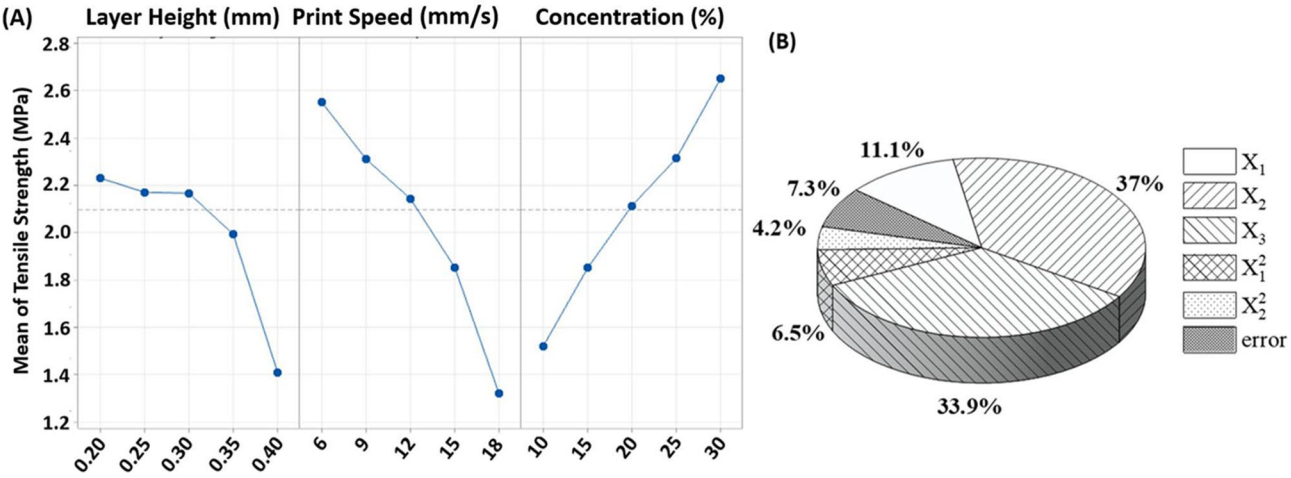

Fig. 4 Impact of 3D printing parameters on tensile strength (**A**) main effect plot and, (**B**) percentage contribution

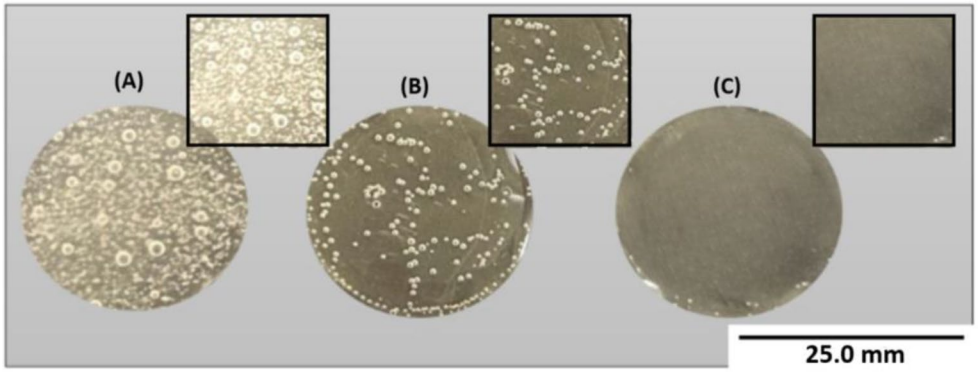

Fig. 5 Demonstration of solvent evaporation related defects in 3D printed samples with different ink concentrations, (**A**) 10 wt%, (**B**) 20 wt% and, (**C**) 30 wt%

Table 6 Response values at optimized process parameters

			Shrinkage (%)		Tensile strength (MPa)	
X_1	X_2	X_3	Statistical	Experimental	Statistical	Experimental
0.25	9.00	30.00	32.33 ± 4.49	34.72	2.98 ± 0.27	2.75

value of tensile strength obtained for the material, which is higher as compared to layer height and ink concentration. As the diffusion between the layers is less it leads to poor mechanical properties. When the print head moves at a relatively lower speed (6 mm/s) there would be a proper deposition of a layer on the print bed which results in better layer-to-layer fusion, hence, the overall strength of the printed material would be higher. The lower print speed provides adequate time for the fusion between the layers. Hence, mechanical strength would be higher when the print speed is lower [38]. Printing with high print speed (18 mm/s), results in thinning of the extruded material raster resulting in defects such as improper fusion which in turn reduces the tensile strength of the 3D printed sample [38].

Influence of ink concentration

The ink concentration significantly affected the physicomechanical quality of the 3D printed specimen. It was identified that parts 3D printed from ink with higher concentration possessed higher tensile strength compared to the parts 3D printed using lower concentration ink. The evaporation of solvent leads to the generation of defects such as micro and macro voids within the sample hence the overall strength of the printed specimen would be reduced. The number of such defects would be dependent upon the solvent content present in the ink. In Fig. 5A it could be seen samples printed with ink having 10wt% concentration possessed a higher number of defects associated with solvent evaporation. On the other hand, Fig. 5B and C show the samples printed with 20 and 30wt% ink samples respectively. It was identified that with an increase in polymer content the size as well as the number of defects reduced significantly. The presence of these defects affects the tensile strength. Thus, the sample with 10 wt% content showed significantly lower tensile strength (~1.5 MPa) compared to samples prepared with higher polymer content ink samples (~2.6 MPa).

Multi-objective optimization

A multi-objective optimization problem was formulated based on the generated statistical models for tensile strength and shrinkage. The objectives of the presented problem were to minimise shrinkage and maximise tensile strength. Genetic algorithm (GA) was utilized to obtain the optimized solution for the objectives. The optimization was performed within the constraints imposed by the upper and lower limit of the input process parameters: $0.2 \leq X_1 \leq 0.4$; $6 \leq X_2 \leq 18$ and; $10 \leq X_3 \leq 30$.

Table 6 provides the results of an experiment performed at optimized layer thickness, print speed, and ink concentration. Interestingly, it was found that the experimental results were in good agreement with the predicted results.

Conclusion

The current work focused on statistical modelling and optimization of printing parameters of DIW-based additive manufacturing of thermoplastic elastomeric material based on TPU/GECO blend. Statistical models were developed to demonstrate the influence of print speed, layer height, and ink concentration on the properties of the printed material. Print speed was found to be the highly influential parameter for both shrinkage and tensile strength. An increase in print speed led to an increase in shrinkage for all the concentrations of ink due to the phenomenon of the dragging effect. Layer height also significantly affected the shrinkage, with a

percentage contribution of ∼22%. On the other hand, tensile strength was also significantly affected by ink concentration having a percentage contribution of ∼34%. It was also evident that with an increase in ink concentration, the size and number of defects associated with solvent evaporation reduced significantly. Moreover, it was also observed that these defects also affected the tensile behaviour of the 3D-printed samples. Finally, a genetic algorithm-based multi-objective optimization was performed to identify the optimized 3D printing parameters of the 50TPU/50GECO (w/w) blend. It was found that a layer height of 0.25 mm, a print speed of 9 mm/s, and an ink concentration of 30 wt% were the optimized parameters.

Acknowledgements
PA and AK acknowledges financial support from the Ministry of Human Resource Development (MHRD), India. Shib Shankar Banerjee acknowledges financial support from the Science and Engineering Research Board—Start-up Research Grant (SERB-SRG), India, vide research grant no. RP04369G.

Author contributions
PA: Conceptualization, Methodology, Investigation, Formal analysis, Writing original draft. AK: Conceptualization, Methodology, Investigation, Formal analysis, Writing original draft. PMP: Conceptualization, Supervision, Review & editing. SSB: Conceptualization, Supervision, Resources, Review & editing.

Data availability
No datasets were generated or analysed during the current study.

Declarations

Competing interests
The authors declare no competing interests.

Received: 10 February 2024 / Accepted: 29 March 2024

References

1. S.C. Ligon et al., Polymers for 3D printing and customized additive manufacturing. Chem. Rev. **117**(15), 10212–10290 (2017)
2. P. Awasthi, S.S. Banerjee, Fused deposition modeling of thermoplastic elastomeric materials: challenges and opportunities. Additive Manuf. **46**, 102177 (2021)
3. H. Wu et al., Recent developments in polymers/polymer nanocomposites for additive manufacturing. Prog. Mater. Sci. **111**, 100638 (2020)
4. A. Al Rashid et al., Additive manufacturing of polymer nanocomposites: needs and challenges in materials, processes, and applications. J. Mater. Res. Technol. **14**, 910–941 (2021)
5. S. Salifu et al., Recent development in the additive manufacturing of polymer-based composites for automotive structures—A review. Int. J. Adv. Manuf. Technol. **119**(11–12), 6877–6891 (2022)
6. G.D. Goh et al., Recent progress in additive manufacturing of fiber reinforced polymer composite. Adv. Mater. Technol. **4**(1), 1800271 (2019)
7. J. Jafferson, D. Chatterjee, *A review on polymeric materials in additive manufacturing* Materials Today: Proceedings, 2021. 46: pp. 1349–1365
8. M.A. Sarabia-Vallejos et al., Innovation in Additive Manufacturing using polymers: a Survey on the Technological and Material developments. Polymers. **14**(7), 1351 (2022)
9. N. Verma et al., Development of material extrusion 3D printing compatible tailorable thermoplastic elastomeric materials from acrylonitrile butadiene styrene and styrene-(ethylene-butylene)-styrene block copolymer blends. J. Appl. Polym. Sci. **139**(42), e53039 (2022)
10. V. Monfared et al., A brief review on additive manufacturing of polymeric composites and nanocomposites. Micromachines. **12**(6), 704 (2021)
11. M. Ahmadifar et al., Additive manufacturing of polymer-based composites using fused filament fabrication (FFF): a review. Appl. Compos. Mater. **28**, 1335–1380 (2021)
12. A. Kumar et al., Experimental investigations into additive manufacturing of styrene-ethylene-butylene-styrene block copolymers using solvent cast 3D printing technique. Rapid Prototyp. J., 2023
13. A.D. Mazurchevici, D. Nedelcu, R. Popa, *Additive manufacturing of composite materials by FDM technology: A review* 2020
14. K. Engel, P.A. Kilmartin, O. Diegel, Flexible and multi-material intrinsically conductive polymer devices fabricated via DLP and DIW additive manufacturing techniques. Rapid Prototyp. J. **29**(10), 2164–2175 (2023)
15. X. Peng et al., Integrating digital light processing with direct ink writing for hybrid 3D printing of functional structures and devices. Additive Manuf. **40**, 101911 (2021)
16. D. Zhang et al., Additive manufacturing of thermoelectrics: emerging trends and outlook. ACS Energy Lett. **7**(2), 720–735 (2022)
17. S. Amin, M. Amin, Thermoplastic elastomeric (TPE) materials and their use in outdoor electrical insulation. Rev. Adv. Mater. Sci. **29**(1), 15–30 (2011)
18. R.J. Spontak, N.P. Patel, Thermoplastic elastomers: fundamentals and applications. Curr. Opin. Colloid Interface Sci. **5**(5–6), 333–340 (2000)
19. R. Bonart, Thermoplastic elastomers. Polymer. **20**(11), 1389–1403 (1979)
20. S. Aiswarya, P. Awasthi, S.S. Banerjee, Self-healing thermoplastic elastomeric materials: challenges, opportunities and new approaches. Eur. Polymer J. **181**, 111658 (2022)
21. S.S. Banerjee et al., Nanomechanics and origin of rubber elasticity of novel nanostructured thermoplastic elastomeric blends using atomic force microscopy. Macromol. Chem. Phys. **216**(15), 1666–1674 (2015)
22. A. Fazli, D. Rodrigue, Waste rubber recycling: a review on the evolution and properties of thermoplastic elastomers. Materials. **13**(3), 782 (2020)
23. P. Awasthi, S.S. Banerjee, Design of ultrastretchable and super-elastic tailorable hydrophilic thermoplastic elastomeric materials. Polymer. **252**, 124914 (2022)
24. G. Holden, E. Bishop, N.R. Legge, *Thermoplastic elastomers*. in *Journal of Polymer Science Part C: Polymer Symposia*. 1969. Wiley Online Library
25. S.S. Banerjee, A.K. Bhowmick, Tailored nanostructured thermoplastic elastomers from polypropylene and fluoroelastomer: morphology and functional properties. Ind. Eng. Chem. Res. **54**(33), 8137–8146 (2015)
26. N.R. Legge, Thermoplastic elastomers. Rubber Chem. Technol. **60**(3), 83–117 (1987)
27. B.P. Grady, S.L. Cooper, Thermoplastic elastomers, *Science and Technology of Rubber*. 1994, Elsevier. 601–674
28. R.J. Cella, *Morphology of segmented polyester thermoplastic elastomers*. in *Journal of Polymer Science: Polymer Symposia*. 1973. Wiley Online Library
29. P. Awasthi, K.A. Pandey, P.M. Banerjee, SS, *Direct Ink Writing based Additive Manufacturing of Thermoplastic Elastomeric Materials* Polymer-Plastics Technology and Materials., 2024
30. R. Kandi, P.M. Pandey, *Statistical modelling and optimization of print quality and mechanical properties of customized tubular scaffolds fabricated using solvent-based extrusion 3D printing process* Proceedings of the Institution of Mechanical Engineers, Part H: Journal of Engineering in Medicine, 2021. 235(12): pp. 1421–1438
31. N. Kumar et al., The effect of process parameters on tensile behavior of 3D printed flexible parts of ethylene vinyl acetate (EVA). J. Manuf. Process. **35**, 317–326 (2018)
32. N. Ayrilmis, Effect of layer thickness on surface properties of 3D printed materials produced from wood flour/PLA filament. Polym. Test. **71**, 163–166 (2018)
33. W. Peng et al., Effects of FDM-3D printing parameters on mechanical properties and microstructure of CF/PEEK and GF/PEEK. Chin. J. Aeronaut. **34**(9), 236–246 (2021)
34. J. Singh et al., A comparative analysis of solvent cast 3D printed carbonyl iron powder reinforced polycaprolactone polymeric stents for intravascular applications. J. Biomedical Mater. Res. Part. B: Appl. Biomaterials. **109**(9), 1344–1359 (2021)
35. B.S. Tomar, A. Shahin, M.S. Tirumkudulu, Cracking in drying films of polymer solutions. Soft Matter. **16**(14), 3476–3484 (2020)
36. A. Kumar et al., Experimental investigations into additive manufacturing of styrene-ethylene-butylene-styrene block copolymers using solvent cast 3D printing technique. Rapid Prototyp. J. **29**(7), 1367–1385 (2023)
37. D.C. Montgomery, *Design and Analysis of Experiments* (Wiley, 2017)

38. J. Singh, G. Singh, P.M. Pandey, Multi-objective optimization of solvent cast 3D printing process parameters for fabrication of biodegradable composite stents. Int. J. Adv. Manuf. Technol. **115**(11–12), 3945–3964 (2021)
39. Y. Jin, W. Chai, Y. Huang, Printability study of hydrogel solution extrusion in nanoclay yield-stress bath during printing-then-gelation biofabrication. Mater. Sci. Engineering: C **80**, 313–325 (2017)
40. S.-Z. Guo, M.-C. Heuzey, D. Therriault, Properties of polylactide inks for solvent-cast printing of three-dimensional freeform microstructures. Langmuir. **30**(4), 1142–1150 (2014)
41. A. Guerra, A. Roca, J. de Ciurana, A novel 3D additive manufacturing machine to biodegradable stents. Procedia Manuf. **13**, 718–723 (2017)
42. Q. Xue et al., *3D-Printed Thermoplastic Polyurethane Filaments with Carbon Nanotubes for Sensing Applications*. in *2023 International Workshop on Impedance Spectroscopy (IWIS)*. 2023. IEEE
43. M.S. Uddin et al., Evaluating mechanical properties and failure mechanisms of fused deposition modeling acrylonitrile butadiene styrene parts. J. Manuf. Sci. Eng. **139**(8), 081018 (2017)

Publisher's Note